Image reconstruction in quantitative photoacoustic tomography using adaptive optical Monte Carlo

Niko Hänninen, Aki Pulkkinen, Simon Arridge, Tanja Tarvainen

Niko Hänninen, Aki Pulkkinen, Simon Arridge, Tanja Tarvainen, "Image reconstruction in quantitative photoacoustic tomography using adaptive optical Monte Carlo," Proc. SPIE 12379, Photons Plus Ultrasound: Imaging and Sensing 2023, 1237916 (9 March 2023); doi: 10.1117/12.2647252

SPIE.

Event: SPIE BiOS, 2023, San Francisco, California, United States

Image reconstruction in quantitative photoacoustic tomography using adaptive optical Monte Carlo

Niko Hänninen[a], Aki Pulkkinen[a], Simon Arridge[b], and Tanja Tarvainen[a, b]

[a]Department of Technical Physics, University of Eastern Finland, Yliopistonranta 1, P.O. Box 1627, 70211 Kuopio, Finland
[b]Department of Computer Science, University College London, Gower Street WC1E 6BT, London, United Kingdom

ABSTRACT

In quantitative photoacoustic tomography (QPAT), distributions of optical parameters inside the target are reconstructed from photoacoustic images. In this work, we utilize the Monte Carlo (MC) method for light transport in the image reconstruction of QPAT. Modeling light transport accurately with the MC requires simulating a large number of photon packets, which can be computationally expensive. On the other hand, too low number of photon packets results in a high level of stochastic noise, which can lead to significant errors in reconstructed images. In this work, we use an adaptive approach, where the number of simulated photon packets is adjusted during an iterative image reconstruction. It is based on a norm test where the expected relative error of the minimization direction is controlled. The adaptive approach automatically determines the number of simulated photon packets to provide sufficiently accurate light transport modeling without unnecessary computational burden. The presented approach is studied with two-dimensional simulations.

Keywords: quantitative photoacoustic tomography, Monte Carlo method for light transport, stochastic optimization

1. INTRODUCTION

In photoacoustic tomography (PAT), the aim is to reconstruct images of the initial pressure distribution generated by absorption of externally introduced light pulse. It can be used, for example, to image blood vessels, microsvasculature of tumors and small animals.[1,2] In quantitative photoacoustic tomography (QPAT), the aim is to estimate concentrations of light absorbing molecules,[3] which provides quantitative information of the target.

Image reconstruction problem of QPAT is an ill-posed inverse problem. An iterative solving of the related minimization problem requires modeling light transport and solving a search direction of the minimization algorithm on each iteration. A widely accepted model for light transport in a scattering medium is the radiative transfer equation (RTE).[4] While the RTE has been previously utilized in QPAT,[5–9] approximating the solution of the RTE numerically for example by a finite element method can be computationally challenging. Alternatively, light transport in biological tissues can be simulated with the Monte Carlo (MC) method for light transport. In MC, light transport is simulated by tracing a large number of photons or photon packets.[10,11] It has been widely utilized in the field of biomedical optics,[12,13] and recently it has been utilized in QPAT.[14–19]

Due to its stochastic nature, the solution given by MC simulation is corrupted by a stochastic noise. The effect of the stochastic noise can be made negligible in practice by simulating a very large number of photon packets, but it can be computationally expensive. On the other hand, reducing the number of photon packets reduces the computational cost. However, using a too low number of photon packets can result in a high level of stochastic noise. This can lead to significant errors in the solution of the inverse problem.

In this work, we approach the QPAT inverse problem in the framework of Bayesian inverse problems.[20,21] The image reconstruction problem is formulated as a minimization problem, that is solved utilizing a stochastic Gauss-Newton (SGN) method. The number of photon packets during the iterative image reconstruction process is determined by a norm test.[15,16,22]

Further author information: (Send correspondence to N.H.)
N.H.: E-mail: niko.hanninen@uef.fi

Photons Plus Ultrasound: Imaging and Sensing 2023, edited by Alexander A. Oraevsky, Lihong V. Wang, Proc. of SPIE Vol. 12379, 1237916 · © 2023 SPIE
1605-7422 · doi: 10.1117/12.2647252

2. LIGHT TRANSPORT MODEL

In the forward problem of QPAT, the absorbed optical energy density H inside the target is solved when the optical parameters and input light are given. Let us consider a domain $\Omega \subset \mathbb{R}^d$ with a boundary $\partial\Omega$ in dimension $d = 2, 3$ and let $\hat{s} \in S^{d-1}$ denote a unit vector in the direction of interest. In QPAT, light propagation can be modelled using the RTE

$$\begin{cases} \hat{s} \cdot \nabla\phi(r,\hat{s}) + (\mu_{\mathrm{s}}(r) + \mu_{\mathrm{a}}(r))\phi(r,\hat{s}) = \mu_{\mathrm{s}}(r) \displaystyle\int_{S^{d-1}} \Theta(\hat{s}\cdot\hat{s}')\phi(r,\hat{s}')\mathrm{d}\hat{s}', \quad r \in \Omega \\ \phi(r,\hat{s}) = \begin{cases} \phi_0(r,\hat{s}), & r \in \epsilon,\ \hat{s}\cdot\hat{n} < 0 \\ 0, & r \in \partial\Omega \setminus \epsilon,\ \hat{s}\cdot\hat{n} < 0 \end{cases} \end{cases} \tag{1}$$

where r is the spatial position, $\mu_{\mathrm{a}}(r)$ is the optical absorption coefficient, $\mu_{\mathrm{s}}(r)$ is the optical scattering coefficient, $\phi(r,\hat{s})$ is the radiance, $\phi_0(r,\hat{s})$ is a boundary source defined at source locations $\epsilon \subset \partial\Omega$, $\hat{n}$ is an outward unit normal, and $\Theta(\hat{s}\cdot\hat{s}')$ is the scattering phase function.[4,23,24] A widely used scattering phase function is the Henyey-Greenstein phase function

$$\Theta(\hat{s}\cdot\hat{s}') = \begin{cases} \frac{1}{2\pi}\frac{1-g^2}{1+g^2-2g\hat{s}\cdot\hat{s}'}, & d = 2 \\ \frac{1}{4\pi}\frac{1-g^2}{(1+g^2-2g\hat{s}\cdot\hat{s}')^{3/2}}, & d = 3 \end{cases}, \tag{2}$$

where $g \in (-1, 1)$ is the scattering anisotropy parameter.[25]

The photon fluence $\Phi(r)$ is obtained from the radiance by

$$\Phi(r) = \int_{S^{d-1}} \phi(r,\hat{s})\mathrm{d}\hat{s}. \tag{3}$$

As light propagates within the medium, it is absorbed by light absorbing molecules (chromophores), creating absorbed optical energy density $H(r)$

$$H(r) = \mu_{\mathrm{a}}(r)\Phi(r). \tag{4}$$

In this work, the MC method is used to approximate the solution of the RTE.[10,11] We use the photon packet method, where light transport is approximated by tracing paths of photon packets in a scattering medium while continuously reducing the weights of the packets to simulate absorption.[10]

3. INVERSE PROBLEM

In the inverse problem of QPAT, optical parameters of the target are estimated from the absorbed energy density H. In this work, we estimate the absorption coefficient μ_{a}, and assume that the scattering coefficient is known. Let us consider an observation model

$$y = f(x) + e, \tag{5}$$

where $y = [H_1, H_2, ..., H_M] \in \mathbb{R}^M$ is the data, $x = \mu_{\mathrm{a}} = [\mu_{\mathrm{a}_1}, \mu_{\mathrm{a}_2}, ..., \mu_{\mathrm{a}_N}] \in \mathbb{R}^N$ denotes the unknown optical absorption coefficients, $f : \mathbb{R}^N \mapsto \mathbb{R}^M$ is the discretized forward model, $e \in \mathbb{R}^M$ is the measurement noise, N is the number of discretization elements in the parameter mesh and M is the number of data points. In this work, we approach the inverse problem in the Bayesian framework.[5,20] In the Bayesian approach, parameters x, y and e are considered as random variables, and the solution to the inverse problem is the posterior distribution $\pi(x|y)$. Solving the full posterior distribution is often computationally too expensive in a tomographic imaging setting. Thus, point estimates, such as *maximum a posteriori* (MAP) estimates, are computed. With Gaussian models for the unknown parameters x and noise e, computing the MAP estimates can be formulated as a minimization problem

$$\hat{x} = \arg\min_x \left\{ \frac{1}{2}||L_e(y - f(x) - \eta_e)||^2 + \frac{1}{2}||L_x(x - \eta_x)||^2 \right\}, \tag{6}$$

where η_e and η_x are the means of the noise and the prior distribution of the optical parameters, respectively, and $L_e^{\mathrm{T}}L_e = \Gamma_e^{-1}$ and $L_x^{\mathrm{T}}L_x = \Gamma_x^{-1}$ are the Cholesky factors of the inverse of the noise and the prior covariance matrices Γ_e and Γ_x, respectively.

3.1 Stochastic Gauss-Newton method

Minimization problem (6) can be solved using methods of numerical optimization, such as the Gauss-Newton method.[26] In the Gauss-Newton method, the forward model $f(x)$ and its Jacobian need to be evaluated on each iteration. However, with MC based forward model, only stochastic approximations of the forward model and its Jacobian can be obtained.

In this work, the optimization problem (6) is approached in the framework of stochastic optimization. That is, we consider that the forward model and its Jacobian given by the MC method are corrupted by a stochastic noise. They can be expressed as

$$f_P(x) = f(x) + \epsilon_f \tag{7}$$
$$J_P(x) = J(x) + \epsilon_J, \tag{8}$$

where $f_P(x)$ is the forward model evaluated with P photon packets at x and $J_P(x)$ is the corresponding Jacobian. Further, $f(x)$ and $J(x)$ are the 'accurate' forward model and its Jacobian, which refer to the (unavailable) asymptotic limit of MC with infinite number of photon packets, and ϵ_f and ϵ_J are stochastic noise in the forward model and its Jacobian, respectively. These approximations are assumed to be unbiased, that is $\mathbb{E}[f_P(x)] = f(x)$ and $\mathbb{E}[J_P(x)] = J(x)$ where $\mathbb{E}$ denotes the expected value.

We utilize a stochastic Gauss-Newton (SGN) method to solve the optimization problem (6). The SGN is a stochastic counterpart of the regular Gauss-Newton method.[26] In SGN method, estimates of x are updated iteratively by

$$x_{i+1} = x_i + \alpha_i G_{P_i}(x_i), \tag{9}$$

where α_i is the step length parameter and the minimization direction $G_{P_i}(x_i)$ is solved from

$$(J_{P_i}^{\mathrm{T}}(x_i)\Gamma_e^{-1}J_{P_i}(x_i) + \Gamma_x^{-1})G_{P_i}(x_i) = J_{P_i}^{\mathrm{T}}(x_i)\Gamma_e^{-1}(y - f_{P_i}(x_i) - \eta_e) - \Gamma_x^{-1}(x_i - \eta_x). \tag{10}$$

where $f_{P_i}(x_i)$ is the forward model evaluated at x_i with P_i photon packets and $J_{P_i}(x_i)$ is its Jacobian. The derivatives of the forward model $f(x)$ with respect to the absorption coefficient can be evaluated during computation of the absorbed energy density in MC simulation, for details, see Refs.[14,15]

3.2 Adaptive Approach

The minimization direction $G_{P_i}(x_i)$ in the SGN method (9)-(10) is evaluated using stochastic approximations of the forward model and its Jacobian. Consequently, the SGN direction is also corrupted by stochastic noise, and the level of this noise depends on the number of simulated photon packets. Thus, the effect of the stochastic noise in the SGN search direction can be controlled by adjusting the number of simulated photon packets.

In this work, we utilize an adaptive approach where the number of photon packets is adjusted during the SGN algorithm.[15] In the adaptive approach, the number of photon packets is determined by a norm test.[15,16,22] In the norm test, the expected relative error of the minimization direction is controlled. The norm test can be expressed as

$$V_{\mathrm{GN}}^2(x) = \frac{\mathbb{E}\left\{||G_{P_i}(x) - G(x)||^2\right\}}{||G(x)||^2} < \gamma^2, \tag{11}$$

where $G(x)$ is the accurate SGN direction and γ is a threshold parameter, describing acceptable error in the minimization direction. In practice, the expected value in the norm test can be evaluated using sample mean and a set of L runs of the MC-based forward model and its Jacobian matrices with P_i photon packets. Furthermore, since the accurate direction $G(x)$ is not available, it can be approximated by using sample means. For details of the methodology and the SGN algorithm, see Ref.[15]

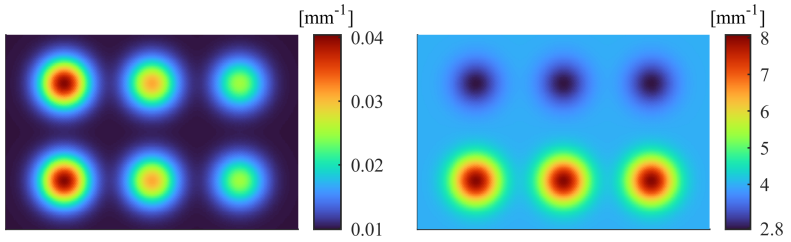

Figure 1. True absorption (left) and scattering (right) distribution presented in the simulation discretization.

4. SIMULATIONS

The adaptive SGN approach was studied with two-dimensional numerical simulations in a rectangular domain of size 15 mm $\times$ 10 mm. The absorption and scattering coefficients that were used to simulate the absorbed optical energy density used as the data y are presented in Fig. 1. Further, anisotropy parameter $g = 0.8$ was used. The data was simulated using four planar illuminations with a uniform density on each side of the domain. The absorbed optical energy density was simulated using the MC method as described in Sec. 2 in a piecewise constant triangular discretization composed of 46142 elements and 23350 nodes. The simulated absorbed optical energy density was then interpolated to a reconstruction discretization to avoid making an inverse crime. After the interpolation, Gaussian random noise with zero mean and standard deviation corresponding to 1% of the maximum value of the noiseless signal was added to the data.

In the inverse problem, absorption coefficient μ_a was estimated from the simulated absorbed optical energy density. The scattering coefficient and anisotropy parameter were assumed to be known. The estimates were computed by minimizing Eq. (6). Two different approaches were studied: an adaptive stochastic Gauss-Newton approach (A-SGN), where the number of photon packets was determined by the norm test approach Eq. (11), and a simple stochastic Gauss-Newton approach (S-SGN), where the number of photon packets was fixed.

In the A-SGN approach, the initial number of photon packets was 100. The norm test was evaluated on every iteration with $L = 10$ samples and with a threshold parameter $\gamma = 0.8$. The S-SGN estimates were computed using 10^3, 10^6 and 10^7 photon packets, which are referred to as S-SGN$_1$, S-SGN$_2$ and S-SGN$_3$, respectively. The S-SGN$_1$ approach corresponds to a case where the number of photon packets is too low to provide accurate reconstructions, while the S-SGN$_3$ corresponds to a case where the number of photon packets is unnecessarily large. The S-SGN$_2$ approach corresponds to a feasible compromise. Estimates were computed in multiple piecewise constant reconstruction discretizations $\mathcal{M}_i$. The number of elements and nodes in the discretizations $\mathcal{M}_i$ are presented in Table 1.

In this work, the prior model of the minimization problem (6) was based on a Gaussian prior with the Ornstein-Uhlenbeck covariance[27] defined as

$$\Gamma_x = \sigma^2 \Xi, \tag{12}$$

Table 1. Number of elements N_e and nodes N_n in the reconstruction discretizations $\mathcal{M}_i$.

	N_e	N_n
$\mathcal{M}_1$	192	117
$\mathcal{M}_2$	374	216
$\mathcal{M}_3$	690	384
$\mathcal{M}_4$	1102	600
$\mathcal{M}_5$	1564	840
$\mathcal{M}_6$	2080	1107

	N_e	N_n
$\mathcal{M}_7$	2760	1457
$\mathcal{M}_8$	3468	1820
$\mathcal{M}_9$	4332	2262
$\mathcal{M}_{10}$	5292	2752
$\mathcal{M}_{11}$	6120	3174
$\mathcal{M}_{12}$	7252	3750

	N_e	N_n
$\mathcal{M}_{13}$	8480	4374
$\mathcal{M}_{14}$	9690	4988
$\mathcal{M}_{15}$	11102	5704
$\mathcal{M}_{16}$	12416	6370
$\mathcal{M}_{17}$	13872	7107
$\mathcal{M}_{18}$	15552	7957

where σ is the standard deviation of the prior and Ξ is defined by its elements as

$$\Xi(i,j) = \exp(-||r_i - r_j||/\tau), \tag{13}$$

where r_i and r_j denote the coordinates of discretization points i and j, respectively, and τ is the characteristic length scale parameter. In the simulations, the optical absorption coefficient was assumed to be within an interval $[\min(\mu_{\mathrm{a}}^{\mathrm{sim}}), \max(\mu_{\mathrm{a}}^{\mathrm{sim}})]$, where $\mu_{\mathrm{a}}^{\mathrm{sim}}$ is the simulated (true) absorption distribution. The mean of the prior distribution η_x was chosen to be the mean of that interval, and the standard deviation was chosen such that $\sigma = 1/6(\max(\mu_{\mathrm{a}}^{\mathrm{sim}}) - \min(\mu_{\mathrm{a}}^{\mathrm{sim}}))$. Furthermore, characteristic length scale of $\tau = 2.5$ mm was used. In the additive noise model, the simulated noise level was used.

In the SGN algorithm, a constant step size parameter $\alpha_i = 1$ was used in all simulations. In all approaches, the initial value x_1 was chosen to be the mean of the prior distribution. The algorithms were assumed to be converged when the relative difference between the last and the previous three estimates was less than 10%.

The results were compared visually and by computing the relative error of the estimates. The relative error was computed by

$$E = 100\% \cdot \frac{||\hat{x} - x^{\mathrm{sim}}||}{||x^{\mathrm{sim}}||}, \tag{14}$$

where $\hat{x}$ is the MAP estimate and x^{sim} is the simulated (true) absorption coefficient interpolated to the reconstruction mesh. Thus, x^{sim} can be considered to be the most accurate representation of the true distribution in that discretization.

5. RESULTS

The true absorption distributions interpolated to the reconstruction meshes and the estimates computed with A-SGN and S-SGN approaches in five different reconstruction meshes are presented in Fig. 2. In the mesh with the smallest number of elements, all the estimates look visually similar. However, when the number of elements increase, the effect of the stochastic noise in the S-SGN$_1$ estimates, where the number of photon packets was low, become clearly visible. All other estimates are visually identical in all of the meshes.

The relative errors of estimates and total number of simulated photon packets with different approaches in different discretizations are presented in Fig. 3. As it can be seen, the relative errors of the S-SGN$_1$ are significantly higher compared to the other approaches, and there is significant variance in the errors due to the stochastic noise. Moreover, the relative error of the S-SGN$_1$ estimates increase as the number of elements increase. This is caused by photon packet statistics: as the number of mesh elements increase, probability that a photon packet goes through a specific mesh element decreases. Thus, less photon packets contribute to the photon propagation and absorption in that element, resulting in more stochastic noise.

The S-SGN$_3$ and A-SGN approach provide estimates with almost identical level of relative error. The S-SGN$_2$ approach provides similar level of relative error with a very low number of mesh elements, but the errors increase as the number of mesh element increase.

In general, the total number of simulated photon packets in the A-SGN approach is in the same scale compared to the S-SGN$_2$ approach. However, as the number of mesh elements increase, the A-SGN approach automatically adjusts the number of photon packets, which increases the number of photon packets in the meshes with high number of elements. More importantly, while the A-SGN and S-SGN$_3$ approaches provide almost identical results, the A-SGN approach requires significantly less photon packets than the S-SGN$_3$ approach in all discretizations.

6. DISCUSSION AND CONCLUSIONS

In this work, the inverse problem of QPAT was studied. Light transport was modeled using the MC method, and the inverse problem was solved in the Bayesian framework utilizing a stochastic Gauss-Newton method. An adaptive approach, where the number of simulated photon packets was adjusted during the iterative image reconstruction, was utilized. The adaptive approach was based on a norm test, where the expected relative error of the minimization direction was controlled.

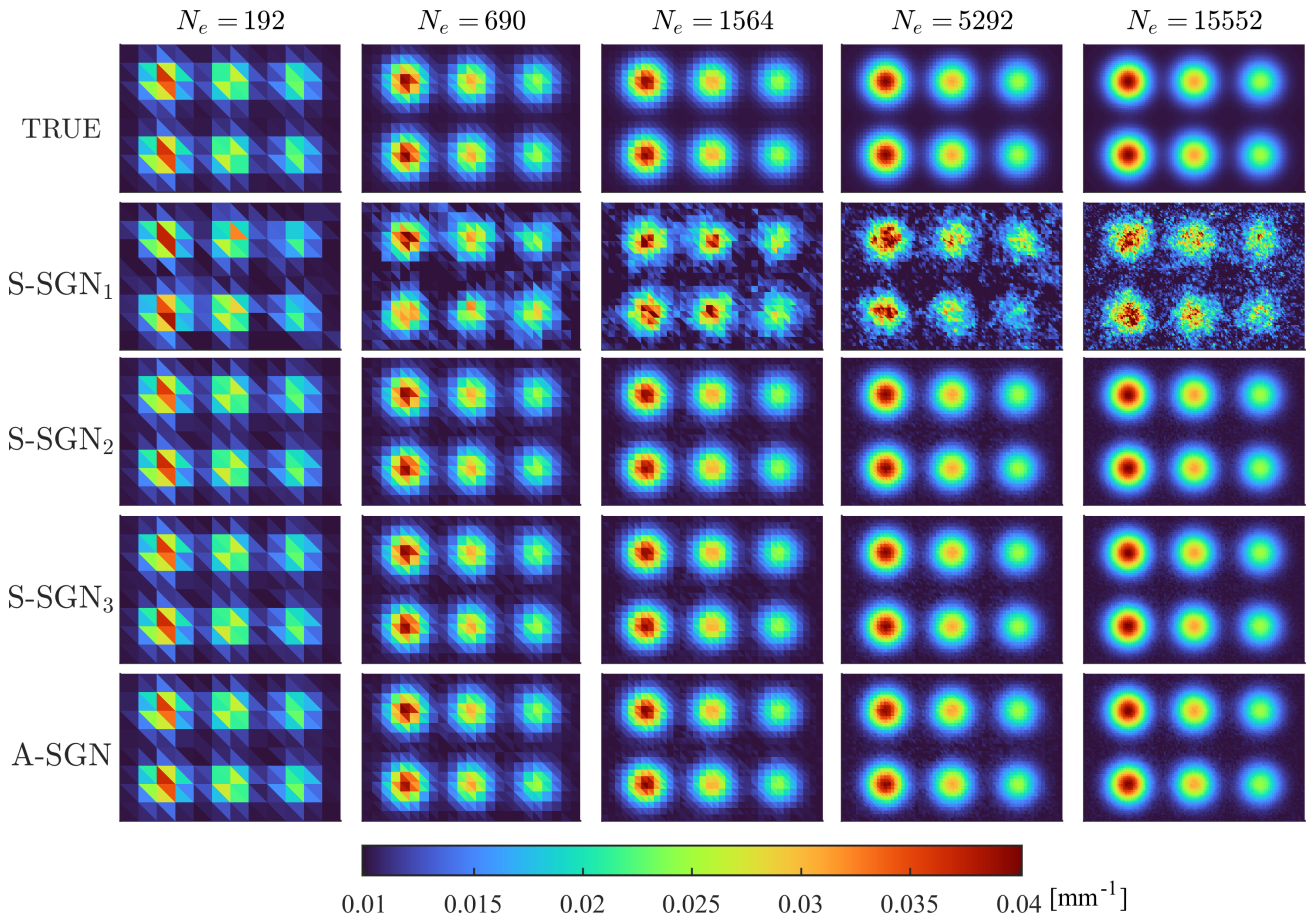

Figure 2. Simulated absorption distribution interpolated to the reconstruction meshes (first row), estimates computed with S-SGN$_1$ approach (second row), S-SGN$_2$ approach (third row), S-SGN$_3$ approach (fourth row) and A-SGN approach (fifth row). Results are shown in a reconstruction meshes with 192 elements (first column), 690 elements (second column), 1564 elements (third column), 5292 elements (fourth column) and 15552 elements (fifth column).

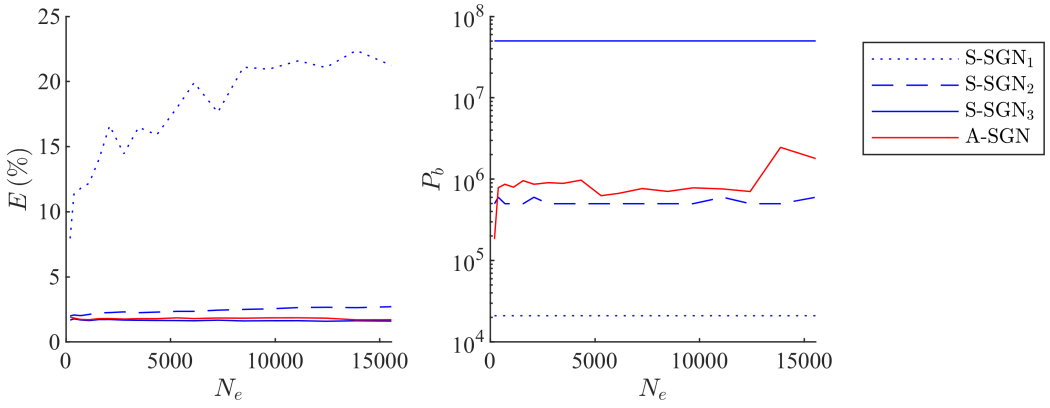

Figure 3. Relative errors of the final estimates E (%) (left) and total number of simulated photon packets P_b (right) with different number of mesh elements N_e with S-SGN$_1$ approach (blue, dotted), S-SGN$_2$ approach (blue, dashed), S-SGN$_3$ approach (blue, solid) and A-SGN approach (red, solid).

As seen in the simulations, using a too low number of photon packets during the image reconstruction resulted in inaccurate reconstructions. On the other hand, choosing a very large number of photon packets resulted in excessive computational cost without any significant improvement in the estimates. Further, with fixed number of photon packets, the relative error of the estimates increased as the number of elements in the reconstruction meshes increased. The adaptive approach studied in this work provided accurate reconstructions in every discretization due to automatically adjusting the number of photon packets. Further, the adaptive approach required significantly fewer photon packets to converge compared to an approach with very large number of photon packets while providing the same accuracy for the absorption estimates.

While the adaptive approach determines the number of photon packets automatically, it requires choosing multiple parameters: the threshold parameter, number of samples used in the test and how often the test is evaluated. In the simulations of this work, the same threshold parameter was observed to provide sufficient accuracy in all discretizations. However, other factors, such as optical parameters inside the target or illumination patterns, may have an effect on the choice of the threshold parameter. Additionally, while the adaptive approach can provide computational savings due to decreasing the number of simulated photon packets, evaluating the norm test introduces additional computations due to solving multiple Gauss-Newton directions on each iterations.

In this work, only the absorption coefficient was estimated while the scattering coefficient was assumed to be known. In practice, this is not a realistic assumption. The similar approach could be utilized in solving both the absorption and scattering coefficient simultaneously, although this can be more challenging due to the ill-posedness of the scattering estimation problem. Evaluating the Jacobian matrix of the MC based forward model with respect to the scattering coefficient requires, for example, perturbation Monte Carlo method.[14]

In conclusion, the MC method for light transport can be utilized in QPAT to obtain accurate absorption reconstructions. However, the stochastic nature of the MC introduces additional challenge of choosing the number of photon packets during the image reconstruction. The adaptive approach studied in this work adjusts the number of photon packets to provide sufficiently accurate simulations. Consequently, it can provide computational savings compared to fixing the number of photon packets unnecessarily large.

ACKNOWLEDGEMENTS

This project has received funding from the European Research Council (ERC) under the European Union's Horizon 2020 research and innovation programme (grant agreement No 101001417 - QUANTOM). This work was supported by the Academy of Finland (Center of Excellence in Inverse Modeling and Imaging project 336799, the Flagship Program Photonics Research and Innovation grant 320166 and Competitive funding to strengthen university research profiles, PROFI6, decision number 336119), by Jenny and Antti Wihuri foundation, Väisälä Fund and the Jane and Aatos Erkko Foundation.

REFERENCES

[1] Beard, P., "Biomedical photoacoustic imaging," *Interface Focus* **1**, 602–631 (2011).

[2] Li, C. and Wang, L. V., "Photoacoustic tomography and sensing in biomedicine," *Phys Med Biol* **54**, R59–R97 (2009).

[3] Cox, B., Tarvainen, T., and Arridge, S., "Multiple illumination quantitative photoacoustic tomography using transport and diffusion models," in [*Tomography and Inverse Transport Theory (Contemporary Mathematics)*], Bal, G., Finch, D., Kuchment, P., Schotland, J., Stefanov, P., and Uhlmann, G., eds., **559**, 1–12, American Mathematical Society, Providence (2011).

[4] Ishimaru, A., [*Wave Propagation and Scattering in Random Media*], vol. 1, Academic Press, New York (1978).

[5] Tarvainen, T., Cox, B. T., Kaipio, J. P., and Arridge, S. R., "Reconstructing absorption and scattering distributions in quantitative photoacoustic tomography," *Inv Probl* **28**, 084009 (2012).

[6] Haltmeier, M., Neumann, L., and Rabanser, S., "Single-stage reconstruction algorithm for quantitative photoacoustic tomography," *Inv Probl* **31**, 065005 (2015).

[7] Saratoon, T., Tarvainen, T., Cox, B. T., and Arridge, S. R., "A gradient-based method for quantitative photoacoustic tomography using the radiative transfer equation," *Inv Probl* **29**, 075006 (2013).

[8] Mamonov, A. V. and Ren, K., "Quantitative photoacoustic imaging in radiative transport regime," *Commun Math Sci* **12**, 201–234 (2014).
[9] Yao, L., Sun, Y., and Jiang, H., "Transport-based quantitative photoacoustic tomography: simulations and experiments," *Phys Med Biol* **55**, 1917–1934 (2010).
[10] Prahl, S. A., Keijzer, M., Jacques, S. L., and Welch, J. L., "A Monte Carlo model of light propagation in tissue," in [*SPIE Proceedings of Dosimetry of Laser Radiation in Medicine and Biology*], **IS 5**, 102 – 111 (1989).
[11] Wang, L., Jacques, S. L., and Zheng, L., "MCML — Monte Carlo modeling of light transport in multi-layered tissues," *Comput Methods Programs Biomed* **47**(2), 131–146 (1995).
[12] Sassaroli, A. and Martelli, F., "Equivalence of four Monte Carlo methods for photon migration in turbid media," *J Opt Soc Am A* **29**(10), 2110–2117 (2012).
[13] Zhu, C. and Liu, Q., "Review of Monte Carlo modeling of light transport in tissues," *J Biomed Opt* **18**(5), 050902 (2013).
[14] Leino, A., Lunttila, T., Mozumder, M., Pulkkinen, A., and Tarvainen, T., "Perturbation Monte Carlo method for quantitative photoacoustic tomography," *IEEE Trans Med Imaging* **39**, 2985–2995 (2020).
[15] Hänninen, N., Pulkkinen, A., Arridge, S. R., and Tarvainen, T., "Adaptive stochastic Gauss–Newton method with optical Monte Carlo for quantitative photoacoustic tomography," *J Biomed Opt* **27**(8), 1 – 21 (2022).
[16] Macdonald, C. M., Arridge, S., and Powell, S., "Efficient inversion strategies for estimating optical properties with Monte Carlo radiative transport models," *J Biomed Opt* **25**(8), 085002–13 (2020).
[17] Hochuli, R., Powell, S., Arridge, S., and Cox, B., "Quantitative photoacoustic tomography using forward and adjoint Monte Carlo models of radiance," *J Biomed Opt* **21**(12), 126004 (2016).
[18] Buchmann, J., Kaplan, B. A., Powell, S., Prohaska, S., and Laufer, J., "Three-dimensional quantitative photoacoustic tomography using an adjoint radiance Monte Carlo model and gradient descent," *J Biomed Opt* **24**(6), 1 – 13 (2019).
[19] Buchmann, J., Kaplan, B., Powell, S., Prohaska, S., and Laufer, J., "Quantitative PA tomography of high resolution 3-d images: Experimental validation in a tissue phantom," *Photoacoustics* **17**, 100157 (2020).
[20] Kaipio, J. and Somersalo, E., "Statistical inverse problems: Discretization, model reduction and inverse crimes," *J Comput Appl Math* **198**, 493–504 (2007).
[21] Tarvainen, T., Pulkkinen, A., Cox, B. T., Kaipio, J. P., and Arridge, S. R., "Bayesian image reconstruction in quantitative photoacoustic tomography," *IEEE Trans Med Imag* **32**(12), 2287–2298 (2013).
[22] Byrd, R. H., Chin, G. M., Nocedal, J., and Wu, Y., "Sample size selection in optimization methods for machine learning," *Math Program* **134**, 127–155 (2012).
[23] Arridge, S. R., "Optical tomography in medical imaging," *Inv Probl* **15**, R41–R93 (1999).
[24] Tarvainen, T., Vauhkonen, M., Kolehmainen, V., Arridge, S. R., and Kaipio, J. P., "Coupled radiative transfer equation and diffusion approximation model for photon migration in turbid medium with low-scattering and non-scattering regions," *Phys Med Biol* **50**, 4913–4930 (2005).
[25] Henyey, L. G. and Greenstein, J. L., "Diffuse radiation in the galaxy," *Astrophys J* **93**, 70–83 (1941).
[26] Nocedal, J. and Wright, S. J., [*Numerical Optimization*], Springer (2006).
[27] Rasmussen, C. E. and Williams, C. K. I., [*Gaussian Processes for Machine Learning*], MIT Press (2006).